Interhemispheric asymmetrical change in gray matter volume in patients with unilateral hippocampal sclerosis

Shunji Mugikura[1], Naoko Mori[2], Miyeong Gang[3], Shigenori Kanno[3], Kazutaka Jin[4], Shin-Ichiro Osawa[5], Nobukazu Nakasato[4], Kei Takase[1]

[1]Department of Diagnostic Radiology, Graduate School of Medicine, Tohoku University, Sendai, [2]Department of Radiology, Akita University Graduate School of Medicine, Akita, [3]Departments of Behavioral Neurology and Cognitive Neuroscience, [4]Epileptology, [5]Neurosurgery, Graduate School of Medicine, Tohoku University, Sendai, Japan.

*Corresponding author:
Shunji Mugikura,
Division of Image Statistics,
Tohoku University, Tohoku
Medical Megabank
Organization, Sendai, Miyagi,
Japan.

mugi844@gmail.com

ABSTRACT

Objectives: To clarify the interhemispheric asymmetrical change in gray matter volume (GMV) in unilateral hippocampal sclerosis (HS), we compared changes in GMV relative to normal subjects between the HS and contralateral or non-HS sides.

Material and Methods: Forty-five patients with unilateral HS and 30 healthy subjects were enrolled. We quantified changes in GMV in the patients with HS as compared to GMV in the normal subjects by introducing the Z-score (Z-GMV) in each region or region of interest in unilateral HS. Then, we assessed the asymmetrically decreased regions, that is, regions with significantly higher Z-GMV on the HS side than the contralateral or non-HS side. Z-GMV was calculated according to the two templates of 58 regions per hemisphere covering the whole brain by anatomical automatic labeling (AAL) and 78 regions per cerebral hemisphere using the Anatomy Toolbox.

Results: Seven and four regions in AAL and 17 and 11 regions in Anatomy Toolbox were asymmetrically decreased in the Left Hand Side (LHS) and Right Hand Side (RHS), respectively. Hippocampus and Caudate in AAL, five subregions of the hippocampus (CA1–3, Dentate Gyrus and hippocampus-amygdala-transition-area and 4 extrahippocampal regions including two subregions in amygdala (CM: Centromedial, SF: Superficial), basal forebrain (BF) (Ch4), and thalamus (temporal) in anatomy toolbox were common among LHS and RHS concerning asymmetrically decreased regions.

Conclusion: By introducing Z-GMV, we demonstrated the regions with asymmetrically decreased GMV in LHS and RHS, and found that the hippocampus and extrahippocampal regions, including the BF, were the common asymmetrically decreased regions among LHS and RHS.

Keywords: Epilepsy, Hippocampal sclerosis, Basal forebrain, Voxel-based morphometry, Mesial temporal lobe epilepsy

INTRODUCTION

Hippocampal sclerosis (HS) is one of the most frequent causes of medial temporal lobe epilepsy. The epileptogenicity of HS is often one-sided (unilateral HS) and is categorized as Left hand side (LHS) or Right hand side (RHS).[1,2] In the visual analysis of magnetic resonance imaging (MRI) for unilateral HS, atrophy of the hippocampus and extrahippocampal regions is generally judged compared to the contralateral hemisphere.[3] The previous visual analysis studies reported that atrophy of the extrahippocampal regions was pronounced in the anterior temporal pole,

amygdala, entorhinal cortex, fornix, mammillary body, posterior thalamus, and contralateral cerebellum.[3]

According to studies of gray matter volume(GMV) using voxel-based morphometry (VBM) on MRI of unilateral HS, GMV in the hippocampus and some extrahippocampal regions on the HS side was significantly lower than that in normal subjects (decreased GMV or decreased GMV relative to normal subjects).[4-9] However, a recent meta-analysis of GMV studies in unilateral HS indicated no common regions with decreased GMV between patients with RHS and LHS.[10] This could be related to the following two methodological concerns used in GMV studies in unilateral HS. First, most GMV studies of unilateral HS did not compare GMV between the HS and the contralateral or the non-HS side. Instead, they compared the GMV of the patients of HS with that of normal subjects.[10] Second, most GMV studies of unilateral HS evaluated decreased GMV. However, they did not evaluate increased GMV,[10] although recent studies have reported increased GMV or enlargement of the extrahippocampal regions in the epileptogenic or contralateral hemisphere in medial temporal lobe epilepsy.[11-14] In unilateral HS, we hypothesized that the decrease in GMV on the HS side relative to that in the normal subjects as well as the possible increase in GMV on the non-HS side relative to that in the normal subjects would make the relative decrease in GMV on the HS side in comparison to the non-HS side (interhemispheric asymmetrical change in GMV) more prominent. Therefore, to clarify the interhemispheric asymmetrical change in GMV, we sought to compare GMV changes relative to normal subjects between the HS and non-HS sides concerning decreased and increased GMV.

When we compared GMV between the HS and non-HS sides and evaluated regions with increased and decreased GMV, we should note that the GMV between the left and right regions or regions of interest (ROIs) was significantly different, even in normal subjects.[15] To correct the normal interhemispheric asymmetry in GMV, a Z-score (Z-GMV) was introduced to quantify the decrease and increase in GMV compared with that in normal subjects ($n = 30$) for each region.[16]

Therefore, to clarify the interhemispheric asymmetrical change in GMV in unilateral HS, we sought to compare the Z-GMV in each region between the HS and non-HS sides. Further, we demonstrated the common and different regions with asymmetrically decreased and increased GMV between RHS ($n = 16$) and LHS ($n = 29$).

MATERIAL AND METHODS

Patients

This observational study was approved by the Institutional Review Board of our Institute (No. 2023-4-038) and informed consent from the patients was waived because the data were obtained for clinical purposes. Informed consent was obtained from all healthy subjects for the prospective acquisition of magnetic resonance (MR) images.

At our institution, epilepsy was diagnosed after comprehensive evaluations, including video-electroencephalogram monitoring, formal neuropsychological tests, MRI, and fluorodeoxyglucose positron-emission tomography (FDG-PET).[17,18] 51 consecutive patients with HS between November 2011 and April 2017 were selected for this study based on the following criteria: (i) clinical diagnosis of unilateral mesial temporal lobe epilepsy (MTLE), (ii) identification of unilateral HS on visual analysis of MRI, and (iii) the presence of temporal hypometabolism on the HS side on FDG PET.[19,20]

The criteria for MRI diagnosis of unilateral HS included smaller size and increased signal intensity of the unilateral hippocampus compared to the contralateral hippocampus on T2-weighted images (T2WI) and fluid-attenuated inversion recovery (FLAIR) images.[20] 6 patients (three men and three women) were excluded due to the presence of old focal lesions in the extratemporal areas. Thus, 45 patients with unilateral HS without extratemporal lesions on MRI were included in this study (22 men and 23 women) [Table 1].[20] Thirty age-matched normal subjects were enrolled to calculate the Z score that quantified the decreased or increased GMV change in patients in HS compared to GMV in normal subjects.

MRI

16 RHS and 29 LHS patients underwent 3T-MRI using either the MAGNETOM Trio, A Tim System, Siemens Healthcare GmbH, Erlangen, Germany (Siemens machine) or the Intera Achieva Quasar Dual, Philips Healthcare, Best, the Netherlands (Philips machine). There was no statistically significant difference in which of the two 3TMRI systems, the RHS and LHS patients were assigned to (Fisher's exact test; $P = 0.3484$). 30 age-matched normal subjects underwent MRI with the identical Siemens machine.

The MRI protocol included the following sequences: Axial T2WI and FLAIR imaging parallel to the anteroposterior commissure axis; axial magnetization-prepared rapid gradient echo imaging (3D T1WI) parallel to the long axis of the hippocampus; coronal short T1 inversion recovery; and FLAIR imaging perpendicular to the long axis of the hippocampus. 3D T1W images acquisition parameters were as follows: MAGNETOM Trio: Axial 3D MPRAGE, 0.9 mm thick, no gap, TR 2000 ms, TE 3.1 ms, TI 900 ms, matrix 320×320, FOV 256×240 mm, flip angle 9°; Intera Achieva Quasar Dual: Axial 3D MPRAGE, 1.0 mm thick, no gap, TR 6.6 ms, TE 3.1 ms, TI 872.9 ms, matrix 268×238, FOV 240×213 mm, flip angle 8°.

Table 1: Clinical characteristics of patients with unilateral HS and healthy subjects.

Clinical characteristics	Unilateral HS (*n*=45)		Normal subjects (*n*=30)	*P*-value
	Right HS (*n*=16)	Left HS (*n*=29)		
Age (years)		37.0±14.0	31.8±5.9	0.13
	39.4±9.97	35.6±15.8		0.24
Sex (men/women)		22/23	15/15	1.0
	8/8	14/15		1.0
Age of onset (years)		17.2±12.8	N/A	
	16.9±12.2	17.3±13.4		0.86
Duration of epilepsy (years)		19.8±13.8	N/A	
	22.5±14.0	18.3±13.7		0.31
Surgery for epilepsy (Yes/no)		16/29	N/A	
	5/11	11/18		0.75
IPIs (number of patients)		31	N/A	
	13	18		0.32

HS: Hippocampal sclerosis, IPIs: Initial precipitating incidents, N/A: Not applicable. Age, sex, age of onset, duration of epilepsy, and surgery after comprehensive evaluations were recorded. The duration of epilepsy was defined as the period from the age of onset to the age of hospitalization with a comprehensive evaluation. The significant medical events that occurred before the onset of temporal lobe epilepsy were recorded as initial precipitating incidents. Initial precipitating incidents included febrile seizures, encephalitis/meningitis, closed-head injury, and perinatal event

VBM

All 3D T1W images were processed using statistical parametric mapping (SPM) 12 (Welcome Department of Imaging Neuroscience, London, UK; http://www.fil.ion.ucl.ac.uk/spm/software/spm12/) in MATLAB R2018a (MathWorks, Natick, MA). The 3D T1WI in DICOM format was converted to the NIFTI format, and the images were aligned parallel to the anteroposterior commissure line. Segmentation was performed to create the gray matter, white matter, cerebral spinal fluid, and other tissue volumes with diffeomorphic anatomical registration through exponentiated lie algebra to improve the accuracy of the alignment of the patient's brain image. The segmented volumes were anatomically normalized into the Montreal Neurological Institute space to be modulated and smoothed with an 8 mm full-width half-maximum Gaussian kernel.

Anatomical automatic labeling (AAL) and anatomy toolbox

We measured GMV using the AAL template [Table 2][21] and anatomy toolbox version 3.0 [Table 3][22] by applying a threshold of more than 50% probability of gray matter to the corresponding probability map. AAL includes 58 regions or ROIs on each side, which cover the whole brain based on neuroanatomical names [Table 2]. Anatomy Toolbox includes 78 subregions or ROIs in each cerebral hemisphere, which do not cover the whole cerebral hemisphere but include small and significant regions based on structural and functional imaging studies [Table 3]. In addition to the seven hippocampal subregions, the template includes four in the amygdala, seven

in the thalamus, and two in the basal forebrain (BF). These subregions include extrahippocampal areas reported to be anatomically related to the hippocampus. In this manuscript, general anatomical names begin with lower-case letters, and region of interest (ROI) names on either of the two templates begin with capital letters. For example, the hippocampus and thalamus are anatomical names, while the Hippocampus is the ROI name used in AAL, and Thalamus (temporal) is the ROI name used in the anatomy toolbox.

Z scores of GMV

Previous research has identified significant differences in GMV between the left and right regions (ROIs), even in normal subjects, which is referred to as normal interhemispheric GMV asymmetry.[15] To account for this normal asymmetry, we introduced a Z-score to quantify GMV changes in each ROI for each side in patients with unilateral HS (referred to as Z-GMV) using the following formula:[16]

Z-GMV = (Mean GMV of each ROI on the left and right in healthy subjects – GMV of each ROI on the left and right in patients)/Standard deviation of GMV in each ROI on the left and right in healthy subjects.

In this formula, when calculating the right Z-GMV, GMV values for each ROI are taken from the right side for both healthy subjects and patients. Conversely, for the left Z-GMV, GMV values for each ROI are taken from the left side for both healthy subjects and patients. Z-GMV >0 and <0 in each ROI indicates that GMV is lower and higher in comparison with the normal brain.

Table 2: Regions of interest (ROIs) description of Anatomical Automatic Labeling (AAL).

Anatomical description	ROIs description (n=58)
precentral gyrus	Precentral
superior frontal gyrus	Frontal_Sup
superior frontal gyrus, orbital part	Frontal_Sup_Orb
middle frontal gyrus	Frontal_Mid
middle frontal gyrus, orbital part	Frontal_Mid_Orb
inferior frontal gyrus, opercular part	Frontal_Inf_Oper
inferior frontal gyrus, triangular part	Frontal_Inf_Tri
inferior frontal gyrus, orbital part	Frontal_Inf_Orb
rolandic operculum	Rolandic_Oper
supplementary motor area	Supp_Motor_Area
olfactory cortex	Olfactory
superior frontal gyrus, medial	Frontal_Sup_Medial
medial frontal gyrus, orbital part	Frontal_Med_Orb
gyrus rectus	Rectus
insula	Insula
anterior cingulate gyrus	Cingulum_Ant
middle cingulate gyrus	Cingulum_Mid
posterior cingulate gyrus	Cingulum_Post
hippocampus	Hippocampus
parahippocampal gyrus	ParaHippocampal
amygdala	Amygdala
calcarine fissure and surrounding cortex	Calcarine
cuneus	Cuneus
lingual gyrus	Lingual
superior occipital gyrus	Occipital_Sup
middle occipital gyrus	Occipital_Mid
inferior occipital gyrus	Occipital_Inf
fusiform gyrus	Fusiform
postcentral gyrus	Postcentral
superior parietal gyrus	Parietal_Sup
inferior parietal, but supramarginal and angular gyri	Parietal_Inf
supramarginal gyrus	SupraMarginal
angular gyrus	Angular
precuneus	Precuneus
paracentral lobule	Paracentral_Lobule
caudate nucleus	Caudate
putamen	Putamen
pallidum	Pallidum
thalamus	Thalamus
heschl gyrus	Heschl
superior temporal gyrus	Temporal_Sup
temporal pole: superior temporal gyrus	Temporal_Pole_Sup
middle temporal gyrus	Temporal_Mid
middle temporal gyrus	Temporal_Pole_Mid
Inferior temporal gyrus	Temporal_Inf
cerebelum_Crus1	Cerebelum_Crus1
cerebelum_Crus2	Cerebelum_Crus2
cerebelum_3	Cerebelum_3
cerebelum_4_5	Cerebelum_4_5
cerebelum_6	Cerebelum_6
cerebelum_7b	Cerebelum_7b

(Contd...)

Table 2: (*Continued*).

Anatomical description	ROIs description (n=58)
cerebelum_8	Cerebelum_8
cerebelum_9	Cerebelum_9
cerebelum_10	Cerebelum_10
vermis_1_2 9100	Vermis_1_2 9100
vermis_4_5 9120	Vermis_4_5 9120
vermis_7 9140	Vermis_7 9140
vermis_9 9160	Vermis_9 9160

Footnotes: 58 regions of interest (ROIs) in each side which cover the whole brain by Anatomical Automatic Labeling (AAL) template

Table 3: Regions of interest (ROIs) description of Anatomy Toolbox template.

Anatomical description (number of ROIs included)	ROIs description (n=78)
cingulate cortex (4ROIs)	Area s24
	Area 25
	Area s32
	Area 33
amygdala (4ROIs)	Amygdala (AStr)
	Amygdala (CM)
	Amygdala (LB)
	Amygdala (SF)
hippocampus (7ROIs)	CA1 (Hippocampus)
	CA2 (Hippocampus)
	CA3 (Hippocampus)
	DG (Hippocampus)
	Entorhinal Cortex
	Subiculum
	HATA
orbitofrontal cortex (3ROIs)	Area Fo1
	Area Fo2
	Area Fo3
superior parietal lobule (SPL) (7ROIs)	Area 5L (SPL)
	Area 5M (SPL)
	Area 5Ci (SPL)
	Area 7A (SPL)
	Area 7PC (SPL)
	Area 7M (SPL)
	Area 7P (SPL)
inferior parietal lobule (IPL) (7ROIs)	Area PFop (IPL)
	Area PFt (IPL)
	Area PFm (IPL)
	Area PF (IPL)
	Area PFcm (IPL)
	Area PGa (IPL)
	Area PGp (IPL)
intraparietal sulcus (IPS) (3ROIs)	Area hIP1 (IPS)
	Area hIP2 (IPS)
	Area hIP3 (IPS)
Broca's region (BA44/BA 45) (2ROIs)	Area 44
	Area 45

(Contd...)

Table 3: (*Continued*).

Anatomical description (number of ROIs included)	ROIs description (n=78)
parietal operculum/SII (4ROIs)	Area OP1 [SII]
	Area OP2 [PIVC]
	Area OP3 [VS]
	Area OP4 [PV]
motor cortex (2ROIs)	Area 4a
	Area 4p
primary somatosensory cortex (4ROIs)	Area 3a
	Area 3b
	Area 1
	Area 2
primary auditory cortex (4ROIs)	Area TE 1.0
	Area TE 1.1
	Area TE 1.2
	Area TE 3
posterior insula (3ROIs)	Area Ig1
	Area Ig2
	Area Id1
dorsal extrastriate cortex (7ROIs)	Area hOc3v [V3v]
	Area hOc3d [V3d]
	Area hOc4v [V4(v)]
	Area hOc4la
	Area hOc4lp
	Area hOc4d [V3A]
	Area hOc5 [V5/MT]
fusiform gyrus (4ROIs)	Area FG1
	Area FG2
	Area FG3
	Area FG4
frontal pole (2ROIs)	Area Fp1
	Area Fp2
basal forebrain (2ROIs)	BF (Ch 1-3)
	BF (Ch 4)
Broadman area (BA) 17 and BA 18 (V1/V2) (2ROIs)	Area hOc1 [V1]
	Area hOc2 [V2]
thalamus (Thal) (7ROIs)	Thal: Motor
	Thal: Parietal
	Thal: Premotor
	Thal: Somatosensory
	Thal: Prefrontal
	Thal: Visual
	Thal: temporal

Footnotes: 78 subregions or ROIs in each cerebral hemisphere do not cover the whole cerebral hemisphere but include small and significant regions based on structural and functional imaging studies.

Asymmetrically decreased and increased regions

In patients with unilateral HS, we compared Z-GMV in the ROIs defined by the AAL and Anatomy Toolbox between the HS and contralateral sides using a paired t-test. We defined the regions in which Z-GMV was significantly higher or lower on the HS side than the contralateral or non-HS side as asymmetrically decreased or increased regions, respectively.

Common asymmetrically decreased and increased regions

We found common regions between asymmetrically decreased regions in LHS and RHS (common asymmetrically decreased regions). We also found common regions between asymmetrically increased regions in LHS and RHS (common asymmetrically increased regions).

Statistics

A paired *t*-test was used to compare Z-GMV in the 58 ROIs defined by AAL and 78 ROIs defined by the Anatomy Toolbox on the left and right sides. $P < 0.001$ was considered statistically significant. All statistical analyses were performed using JMP Pro 16.0 software (SAS Institute, Cary, NC, USA).

RESULTS

AAL

7 regions were asymmetrically decreased regions in LHS, in which Z-GMVs in the LHS/RHS were significantly higher than that in the right (non-HS side), and three regions were asymmetrically increased regions in LHS, in which Z-GMVs in the left (HS side) were significantly lower than that in the right (non-HS side) [Figure 1a]. Four regions were symmetrically decreased regions in RHS, and one region was asymmetrically increased regions in RHS [Figure 1b].

The common regions between the asymmetrically decreased regions in LHS and those in RHS (common asymmetrically decreased regions) were the Hippocampus and Caudate. In addition to the two common asymmetrically decreased regions, the five extrahippocampal regions including Rolandic_Oper, Frontal_Sup_Medial, Temporal_Pole_Sup, Temporal_Pole_Mid, and Cerebelum_10 constituted asymmetrically decreased regions in LHS [Figure 1a]. In addition to the two common asymmetrically decreased regions, that is, two regions of the Putamen and Pallidum were asymmetrically decreased in the RHS [Figure 1b].

There were no common regions between the asymmetrically increased regions in LHS and RHS. Asymmetrically increased regions in LHS included three regions, Cerebelum_Crus1, Cerebelum_Crus2, and Cerebelum_9 [Figure 1a]. Further, Z-GMVs (mean) were >0 on the right (non-HS side) in such regions.

In most of the asymmetrically decreased regions in both LHS and RHS, the combination of Z-GMV (mean) was >0 on the HS side and <0 on the non-HS side (LHS: Four of seven regions in [Figure 1a] and RHS: Three of four regions in [Figure 1b]).

Anatomy toolbox template (anatomy toolbox)

Seventeen were asymmetrically decreased regions in LHS and the one region, Area 7M (SPL) was an asymmetrically

increased region in LHS [Figure 2a]. Eleven were asymmetrically decreased regions in RHS and the three (Area s32, Area Fo1, and Thalamus: Motor) were asymmetrically increased regions in RHS [Figure 2b].
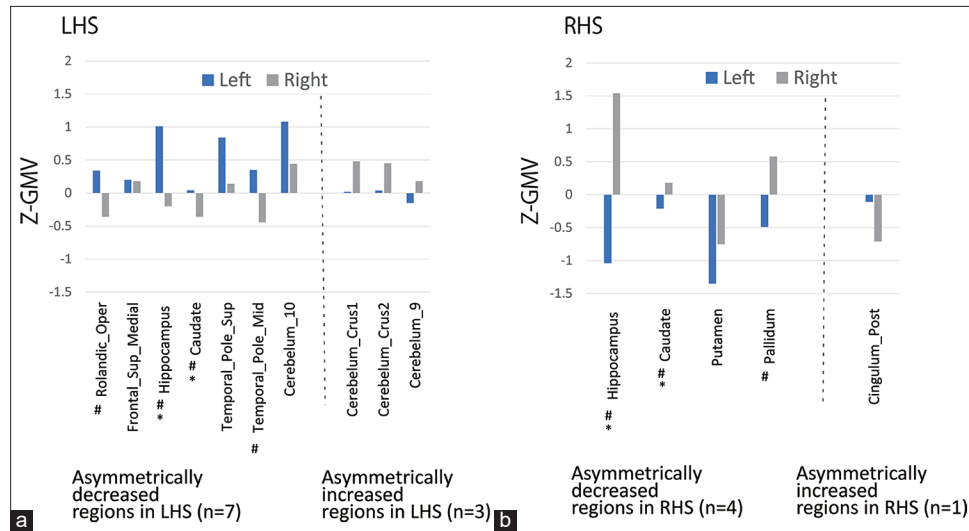
Figure 1: Z-score gray matter volume (Z-GMV) by anatomical automatic labeling template. (a) shows G-GMV (mean) in asymmetrically decreased (*n* = 7) (left of the dotted line) and increased regions in left hippocampal sclerosis (LHS) (*n* = 3) (right of the dotted line). (b) shows G-GMV (mean) in asymmetrically decreased (*n* = 4) (left of the dotted line) and increased regions in the right hippocampal sclerosis (RHS) (*n* = 1) (right of the dotted line). Asterisk (*) indicates the common regions (*n* = 2, Hippocampus and Caudate) between the asymmetrically decreased regions in LHS and RHS (common asymmetrically decreased regions). There were no common regions between the asymmetrically increased regions in LHS and RHS. Sharp (♯) indicates regions in which the Z-GMV (mean) was >0 on the HS side and was <0 on the non-HS side.
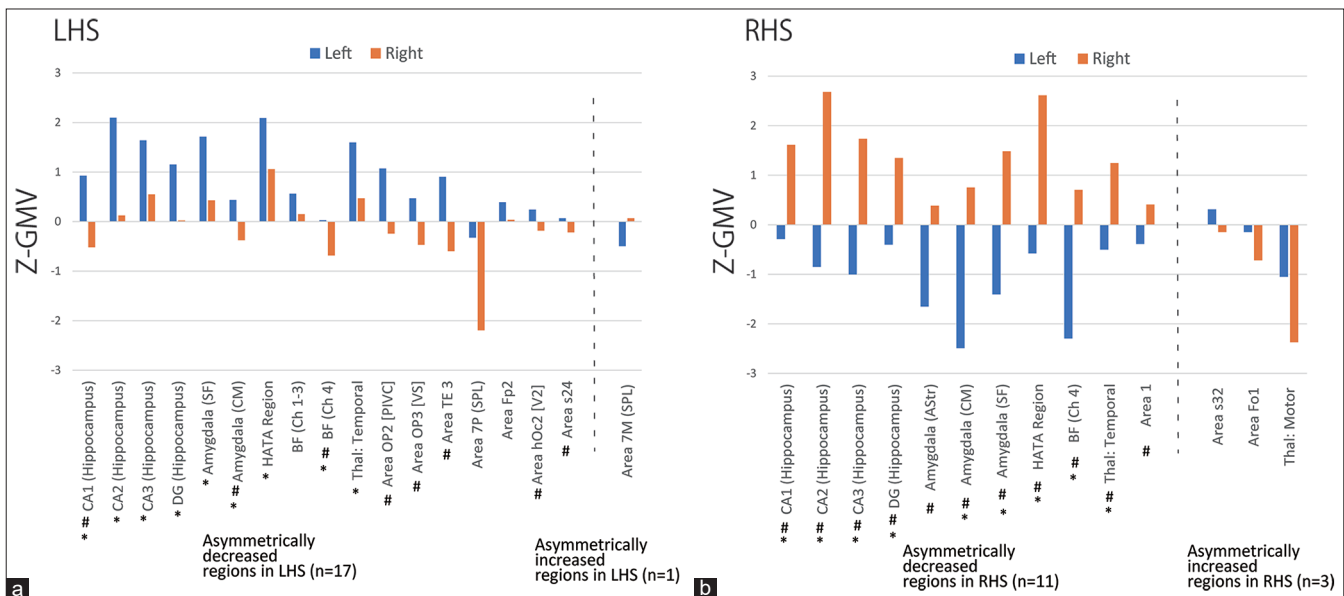
Figure 2: Z-score gray matter volume (Z-GMV) by Anatomy Toolbox template (Anatomy Toolbox). (a) shows Z-GMV (mean) in 17 asymmetrically decreased (left of the dotted line) and one asymmetrically increased region in left hippocampal sclerosis (LHS) (right of the dotted line). (b) shows Z-GMV (mean) in 11 asymmetrically decreased (left of the dotted line) and three asymmetrically increased regions in the right hippocampal sclerosis (RHS) (right of the dotted line). The asterisk (*) indicates the common regions (*n* = 9) between the asymmetrically decreased regions in LHS and RHS (common asymmetrically decreased regions). Sharp (♯) indicates regions in which Z-GMV (mean) was >0 on the HS side and Z-GMV (mean) was <0 on the non-HS side.

Common asymmetrically decreased regions included nine regions of five subregions of the hippocampus, that is, CA1 (hippocampus), CA2 (hippocampus), CA3 (hippocampus), DG (hippocampus), and hippocampal–amygdaloid transition area (HATA), and four extrahippocampal regions, including two subregions of the amygdala, that is, Amygdala (Centromedial [CM]) and Amygdala (Superficial [SF]), basal forebrain (BF)(Ch4), and Thalamus: Temporal.

In addition to the nine common asymmetrically decreased regions, eight extrahippocampal regions constituted asymmetrically decreased regions in LHS [Figure 2a]. In addition to the nine common asymmetrically decreased regions, two extrahippocampal regions constituted asymmetrically decreased regions in the RHS [Figure 2b].

There were no common regions between the asymmetrically increased regions in LHS and RHS. Asymmetrically increased regions in LHS included one extrahippocampal region, that is, Area 7M (SPL) [Figure 2a]. Asymmetrically increased regions in the RHS included three regions, that is, Area s32, Area Fo1, and Thalamus: Motor.

In most of the asymmetrically decreased regions in both LHS and RHS, the combination of Z-GMV (mean) was >0 on the HS side and <0 on the non-HS side (LHS: Eight of 17 regions in [Figure 2a] and RHS: All of 11 regions in [Figure 2b]).

DISCUSSION

To clarify the interhemispheric asymmetrical change in GMV, we introduced Z-GMV and compared it between the HS and non-HS sides. Common asymmetrically decreased regions in LHS and RHS in the AAL included the hippocampus (Hippocampus) and caudate nucleus (Caudate). In the Anatomy Toolbox, the common asymmetrically decreased region included five subregions of the hippocampus (CA1-3, DG, and HATA), and four extrahippocampal regions of two subregions in the amygdala (Amygdala [CM and SF]), one in the BF (BF [Ch4]), and one in the thalamus (Thalamus: Temporal).

The hippocampus as common asymmetrically decreased regions in AAL (Hippocampus) and in the Anatomy Toolbox (CA1-3, DG, and HATA) could agree with MRI diagnostic criteria for LHS and RHS used in this study: to compare the size and signal intensity of the left and right hippocampus by visual evaluation and set the side with smaller and higher T2WI signal intensity to the HS side.

Concerning the extrahippocampal regions, we found that four regions including the amygdala, thalamus, BF, and caudate nucleus common asymmetrically decreased regions in LHS and RHS. The amygdala and thalamus, as whole regions (Amygdala and Thalamus defined by the AAL, respectively) were not included, but the two subregions of the amygdala (Amygdala [CM] and Amygdala [SF]) and one subregion in the thalamus

(Thalamus [temporal]) defined in the Anatomy Toolbox were included in the study. These subregions are understood to interact closely with the hippocampus, as shown in diffusion tensor imaging and static state functional MRI studies.[7,23-25] The BF (Ch4) as defined in the Anatomy Toolbox) was included in common asymmetrically decreased regions in LHS and RHS. We hypothesized that the involvement of the BF (Ch4) and the resulting asymmetric reduction in GMV may be associated with the cognitive decline often observed in unilateral HS. Indeed, the BF, particularly a small region of the basal ganglia of Meynert (Ch4), extends cholinergic fibers to the cerebral hemispheres and plays an important role in the cognitive function of memory; decreased GMV in the BF (Ch4), as measured by VBM, is associated with Alzheimer's disease[26] and Parkinson's disease.[27] The caudate nucleus (Caudate as defined by AAL) as common asymmetrically decreased extrahippocampal regions could be consistent with a recent report showing hypometabolism on FDG-PET of the caudate nucleus on the HS side compared to the non-HS side.[28]

Our study suggested the two characteristics regarding the interhemispheric asymmetrical changes in GMV in patients with unilateral HS. First, more extensive regions were asymmetrically involved in LHS than in RHS, which was already suggested by the previous GMV studies of unilateral HS.[29,30] We were especially interested in the two regions found only in LHS. First, Temporal_Pole_Sup and Temporal_Pole_Mid in AAL were found in LHS as asymmetrically decreased regions but not in RHS. The temporal pole is the area in which atrophy and hyperintensity in the T2-weighted image or FLAIR images are associated with ipsilateral HS as per visual analysis and VBM studies.[31,32] The involvement of the ipsilateral temporal pole associated with unilateral HS, as found in visual analysis or VBM studies, could indicate the possible extrahippocampal epileptogenicity often associated with unilateral HS.[33] Other regions of interest were Cerebelum_Crus1, Cerebelum_Crus2, and Cerebelum_9, which were asymmetrically increased regions in LHS. In such regions, Z-GMV (mean) was >0 in the contralateral HS side (right), indicating that the GMVs were decreased more in the contralateral HS side (right) than in normal subjects. This result could agree with a previous study that showed atrophy of the contralateral cerebellum in visual analysis and VBM.[34]

The second characteristic regarding the interhemispheric asymmetrical changes in GMV in unilateral HS is that among asymmetrically decreased regions in unilateral HS, most of the regions showed the combination of decreased GMV on the HS side compared to healthy controls (Z-GMV [mean]>0) and increased GMV on the non-HS side compared to healthy controls (Z-GMV [mean]<0). Therefore, we suppose that such characteristics could contribute to detecting the common asymmetrically decreased regions in LHS and RHS, by comparing Z-GMVs between the HS side

and the contralateral or non-HS side. In addition, increased GMV on the non-HS side in unilateral HS compared to healthy controls has not been fully explored in the previous reports and should be clarified in larger studies conducted in the future.

The strength of this study is the application of the Anatomy Toolbox in addition to the AAL to compare Z-GMV on the HS and non-HS sides. This enabled us to identify interhemispheric asymmetrical change in GMV in patients with unilateral HS in a small region, mainly in the medial temporal region. Another feature of this study is that we did not use surface-based morphometry (SBM) but VBM, because the evaluation of GMV using VBM is simple and effective when examining interhemispheric asymmetrical change in a small number of cases, as in this study. The GMV is considered a variable that simultaneously represents cortical thickness, and cortical fold, calculated as independent variables in the SBM.[35] Indeed, although a single-center and small study, our Z-GMV results were consistent with those of a recent large multicenter study analyzing gray matter thickness in 732 MTLE patients and 1418 healthy controls using SBM. In this study, the authors introduced an asymmetry index of gray matter thickness with normalized Z-score to quantify gray matter thickness asymmetry.[16] They reported that both the RHS and LHS showed interhemispheric asymmetry centered in the medial temporal lobe as shown in our study.

This study had limitations. First, the number of patients with unilateral HS and healthy subjects was small, and this was a retrospective study that used two different MR scanners. The next limitation is that this study has not analyzed the relationship between the asymmetrically decreased GMV change and the duration or age at seizure onset. We sought to clarify the asymmetrically decreased GMV in unilateral HS between the HS- and non-HS sides in a relatively small number of patients at a single institution, and the duration and age at seizure onset in patients with LHS and RHS did not differ significantly.

CONCLUSION

We suggest the importance of comparing Z-GMV between the HS- and contralateral or non-HS sides in the evaluation of GMV in unilateral HS. We found that the hippocampus and extrahippocampal regions, including the BF, were associated with significantly higher Z-GMV on the HS side than the non-HS side in RHS and LHS.

Ethical approval

This observational study was approved by the Institutional Review Board of our Institute (No. 2023-4-038) and informed consent from the patients was waived because the data were obtained for clinical purposes.

Declaration of patient consent

The authors certify that they have obtained all appropriate patient consent.

Financial support and sponsorship

Nil.

Conflicts of interest

There are no conflicts of interest.

Use of artificial intelligence (AI)-assisted technology for manuscript preparation

The authors confirm that there was no use of artificial intelligence (AI)-assisted technology for assisting in the writing or editing of the manuscript and no images were manipulated using AI.

REFERENCES

1. Masaki H, Watanabe K, Kakeda S, Ide S, Sugimoto K, Ueda I, *et al.* Hippocampal sclerosis without visually detectable hippocampal MRI abnormalities: Automated subfield volumetric analysis. Jpn J Radiol 2020;38:1020-7.
2. Hanamiya M, Korogi Y, Kakeda S, Ohnari N, Kamada K, Moriya J, *et al.* Partial loss of hippocampal striation in medial temporal lobe epilepsy: Pilot evaluation with high-spatial-resolution T2-weighted MR imaging at 3.0 T. Radiology 2009;251:873-81.
3. Urbach H, Mast H, Egger K, Mader I. Presurgical MR imaging in epilepsy. Clin Neuroradiol 2015;25 Suppl 2:151-5.
4. Pell GS, Briellmann RS, Pardoe H, Abbott DF, Jackson GD. Composite voxel-based analysis of volume and T2 relaxometry in temporal lobe epilepsy. Neuroimage 2008;39:1151-61.
5. Tae WS, Joo EY, Kim ST, Hong SB. Gray, white matter concentration changes and their correlation with heterotopic neurons in temporal lobe epilepsy. Korean J Radiol 2010;11:25-36.
6. Bernasconi N, Duchesne S, Janke A, Lerch J, Collins DL, Bernasconi A. Whole-brain voxel-based statistical analysis of gray matter and white matter in temporal lobe epilepsy. Neuroimage 2004;23:717-23.
7. Riederer F, Lanzenberger R, Kaya M, Prayer D, Serles W, Baumgartner C. Network atrophy in temporal lobe epilepsy: A voxel-based morphometry study. Neurology 2008;71:419-25.
8. Pail M, Brázdil M, Marecek R, Mikl M. An optimized voxel-based morphometric study of gray matter changes in patients with left-sided and right-sided mesial temporal lobe epilepsy and hippocampal sclerosis (MTLE/HS). Epilepsia 2010;51:511-8.
9. Bonilha L, Rorden C, Castellano G, Pereira F, Rio PA, Cendes F, *et al.* Voxel-based morphometry reveals gray matter network atrophy in refractory medial temporal lobe epilepsy. Arch Neurol 2004;61:1379-84.
10. Zheng L, Bin G, Zeng H, Zou D, Gao J, Zhang J, *et al.* Meta-analysis of voxel-based morphometry studies of gray matter abnormalities in patients with mesial temporal lobe epilepsy

and unilateral hippocampal sclerosis. Brain Imaging Behav 2018;12:1497-503.

11. Kimura Y, Sato N, Saito Y, Ito K, Kamiya K, Nakata Y, *et al.* Temporal lobe epilepsy with unilateral amygdala enlargement: Morphometric MR analysis with clinical and pathological study. J Neuroimaging 2015;25:175-83.

12. Marcian V, Marecek R, Pail M, Brazdil M. Cerebrocerebellar structural covariance in temporal lobe epilepsy with hippocampal sclerosis. Epilepsy Behav 2020;111:107180.

13. Pereira FR, Alessio A, Sercheli MS, Pedro T, Bilevicius E, Rondina JM, *et al.* Asymmetrical hippocampal connectivity in mesial temporal lobe epilepsy: Evidence from resting state fMRI. BMC Neurosci 2010;11:66.

14. Takaya S, Ikeda A, Mitsueda-Ono T, Matsumoto R, Inouchi M, Namiki C, *et al.* Temporal lobe epilepsy with amygdala enlargement: A morphologic and functional study. J Neuroimaging 2014;24:54-62.

15. Good CD, Johnsrude I, Ashburner J, Henson RN, Friston KJ, Frackowiak RS. Cerebral asymmetry and the effects of sex and handedness on brain structure: A voxel-based morphometric analysis of 465 normal adult human brains. Neuroimage 2001;14:685-700.

16. Park BY, Larivière S, Rodríguez-Cruces R, Royer J, Tavakol S, Wang Y, *et al.* Topographic divergence of atypical cortical asymmetry and atrophy patterns in temporal lobe epilepsy. Brain 2021;145:1285-98.

17. Agari D, Jin K, Kakisaka Y, Kanno A, Ishida M, Kawashima R, *et al.* Magnetoencephalography to confirm epileptiform discharges mimicking small sharp spikes in temporal lobe epilepsy. Clin Neurophysiol 2021;132:1785-9.

18. Suzuki M, Jin K, Kitazawa Y, Fujikawa M, Kakisaka Y, Sato S, *et al.* Diagnostic yield of seizure recordings and neuroimaging in patients with focal epilepsy without interictal epileptiform discharges. Epilepsy Behav 2020;112:107468.

19. Sato S, Iwasaki M, Suzuki H, Mugikura S, Jin K, Tominaga T, *et al.* T2 relaxometry improves detection of non-sclerotic epileptogenic hippocampus. Epilepsy Res 2016;126:1-9.

20. Morishita Y, Mugikura S, Mori N, Tamura H, Sato S, Akashi T, *et al.* Atrophy of the ipsilateral mammillary body in unilateral hippocampal sclerosis shown by thin-slice-reconstructed volumetric analysis. Neuroradiology 2019;61:515-23.

21. Tzourio-Mazoyer N, Landeau B, Papathanassiou D, Crivello F, Etard O, Delcroix N, *et al.* Automated anatomical labeling of activations in SPM using a macroscopic anatomical parcellation of the MNI MRI single-subject brain. Neuroimage 2002;15:273-89.

22. Eickhoff SB, Stephan KE, Mohlberg H, Grefkes C, FinkGR, Amunts K, *et al.* A new SPM toolbox for combining probabilistic cytoarchitectonic maps and functional imaging data. Neuroimage 2005;25:1325-35.

23. Li J, Zhang Z, Shang H. A meta-analysis of voxel-based morphometry studies on unilateral refractory temporal lobe epilepsy. Epilepsy Res 2012;98:97-103.

24. Amunts K, Kedo O, Kindler M, Pieperhoff P, Mohlberg H, Shah NJ, *et al.* Cytoarchitectonic mapping of the human amygdala, hippocampal region and entorhinal cortex: Intersubject variability and probability maps. Anat Embryol (Berl) 2005;210:343-52.

25. Labate A, Cerasa A, Gambardella A, Aguglia U, Quattrone A. Hippocampal and thalamic atrophy in mild temporal lobe epilepsy: A VBM study. Neurology 2008;71:1094-101.

26. Jethwa KD, Dhillon P, Meng D, Auer DP. Alzheimer's Disease Neuroimaging Initiative. Are linear measurements of the nucleus basalis of meynert suitable as a diagnostic biomarker in mild cognitive impairment and Alzheimer's disease? AJNR Am J Neuroradiol 2019;40:2039-44.

27. Gang M, Baba T, Hosokai Y, Nishio Y, Kikuchi A, Hirayama K, *et al.* Clinical and cerebral metabolic changes in Parkinson's disease with basal forebrain atrophy. Mov Disord 2020;35:825-32.

28. Tatekawa H, Uetani H, Hagiwara A, Hotta M, Stern JM, Engel J Jr., *et al.* Association of hypometabolic extension of (18)F-FDG PET with diffusion tensor imaging indices in mesial temporal lobe epilepsy with hippocampal sclerosis. Seizure 2021;88:130-7.

29. Santana MT, Jackowski AP, Britto Fdos S, Sandim GB, Caboclo LO, Centeno RS, *et al.* Gender and hemispheric differences in temporal lobe epilepsy: A VBM study. Seizure 2014;23:274-9.

30. Bonilha L, Alessio A, Rorden C, Baylis G, Damasceno BP, Min LL, *et al.* Extrahippocampal gray matter atrophy and memory impairment in patients with medial temporal lobe epilepsy. Hum Brain Mapp 2007;28:1376-90.

31. Casciato S, Picardi A, D'Aniello A, De Risi M, Grillea G, Quarato PP, *et al.* Temporal pole abnormalities detected by 3 T MRI in temporal lobe epilepsy due to hippocampal sclerosis: No influence on seizure outcome after surgery. Seizure 2017;48:74-8.

32. Wang K, Cao X, Wu D, Liao C, Zhang J, Ji C, *et al.* Magnetic resonance fingerprinting of temporal lobe white matter in mesial temporal lobe epilepsy. Ann Clin Transl Neurol 2019;6:1639-46.

33. Itabashi I, Jin K, Sato S, Suzuki H, Iwasaki M, Kitazawa Y, *et al.* Initial delta and delayed theta/alpha pattern in the temporal region on ictal EEG suggests purely hippocampal epileptogenicity in patients with mesial temporal lobe epilepsy. Clin Neurophysiol 2021;132:737-43.

34. Guo Q, Wei Z, Fan Z, Hu J, Sun B, Jiang S, *et al.* Quantitative analysis of cerebellar lobule morphology and clinical cognitive correlates in refractory temporal lobe epilepsy patients. Epilepsy Behav 2021;114:107553.

35. Goto M, Abe O, Hagiwara A, Fujita S, Kamagata K, Hori M, *et al.* Advantages of using both voxel- and surface-based morphometry in cortical morphology analysis: A review of various applications. Magn Reson Med Sci 2022;21:41-57.